SAW Temperature Sensors with Stable and Robust Electrical Response Versus Environmental Parameters

Marianne Sagnard*[†], Thierry Laroche[†] and Sylvain Ballandras[†]

* Femto-ST - Time and frequency department

[†] Frec'n'sys SAS

emails: marianne.sagnard@frecnsys.fr, thierry.laroche@frecnsys.fr, sylvain.ballandras@frecnsys.fr

Abstract—**Surface acoustic wave (SAW) devices are often used to monitor environmental parameters. In order to ensure the continuity of the frequency response versus these parameters - namely, to remove the effects of directivity, transducers working out of the Bragg conditions are studied. Then, it is shown that the multimodal nature of the acoustic cavity can be exploited to design monolithic temperature SAW sensors.**

Keywords–Surface acoustic wave; SAW; resonators; sensors; temperature; Bragg band; directivity; three strips per wavelength.

I. INTRODUCTION

Physical quantities, such as temperature or pressure need to be monitored in various industry sectors for safety reasons and/or to ensure the good functioning of the facilities. One major issue is that some sensors are inserted in harsh environments and in places where human intervention is not possible. For instance, they could be located in rotary environment (airplane turbines), oven where they face high temperatures (steel industry), or they could also be subject to high magnetic field. Consequently, passive wireless sensors were developed. These sensors make use of piezoelectricity and surface acoustic waves (SAW) to allow remote measurements based on time or frequency [1], [2].

Classically, one of the most common configurations for SAW sensors is made of several resonators. These devices allow for frequency differential measurements by taking into account the behavior of each resonator regarding the quantity of interest [3], [4] (the frequency difference between the minima of the reflexion terms S_{11} is determined). However, two difficulties come up. The first one is a significant issue : how do different resonators interact and age in a different way along time? Secondly, these systems usually work at the Bragg conditions [5]; meaning that electrodes composing the transducer are deposited on the surface of a piezoelectric material so that the resonator is synchronous. Then, directivity properties can be affected by environmental changes and consequently, electrical response can be distorted, leading to the appearance of contributions at the beginning and at the end of Bragg band, to frequency jumps and finally, to wrong measurement interpretations.

The solutions to design SAW wireless and battery-free sensors proposed in this paper aim at resolving the two previous considerations. At first, the stability of the frequency response is ensured thanks to the geometry of the device, which directly impacts the sensitivity of the device to directivity. This assertion is pointed out through different cases. Namely, resonators are usually designed so that they are composed of mirrors to create an acoustic cavity and of a finite transducer whose mechanical period is twice smaller than the electrical period [6]. These resonators work inside the Bragg band and are subject to the previous constraints (risk of frequency jumps when the directivity evolves, interaction between the different resonators composing the structure). Thus, the idea is to modify the design of the transducers in order to make them work out of the Bragg band. The mirrors remain unchanged [7]. Therefore, several SAW structures using langasite (LGS) (YXlt)/48.5/26.7º cut and working out of the Bragg conditions are designed to create acoustic cavity with a prevailing mode. It is shown that resonators that meet the spectral purity requirements can be designed.

Next, the intrinsic multimodal nature of the cavity is used to design a monolithic sensor. By this way, the sensor is free from the aging of each system independently and from the interaction between them. A structure with more than three resonances in the Industrial - Scientific - Medical (ISM) band is designed to bring to light that a differential measurement can be conducted directly between the different modes of the system.

These different elements are pointed out using langasite once again. This choice was made for two reasons. Firstly, LGS was chosen due to the stability of its constants (piezoelectric, elastic,etc.) at high temperatures. It is consequently a good material for high temperature applications. Then, surface acoustic waves on LGS exhibit a low velocity, which allows the shrinking of sensoe dimensions for a given operating frequency.

Finally, experimental measurements are carried out on Quartz devices to emphasize the possibility to measure temperature from 25ºC to at minimum 130ºC with a single resonator sensor and to show the good calculation/test correlation. Quartz was selected for experimental validations thanks to its well-known material constants and because it is quite easy to process compared to materials like langasite.

Consequently, section II details the directivity effects and proposes a method to remove them. Next, section III is devoted to the design of a monolithic SAW sensor by exploiting the multimodal nature of the specific acoustic cavity described in this work. Last part (section IV) concludes draws conclusions on this study.

II. STABILITY OF THE FREQUENCY RESPONSE OF A SAW DEVICE

A. Preliminary assessments

The stability of the frequency response of SAW sensors is a crucial issue in measurement. It has been noticed that the electrical response can be distorted and that frequency jumps can appear when parameters like temperature or pressure vary. This is pointed out on Figure 1, which shows the evolution of the frequency response of a resonator working at the Bragg condition when temperature varies from 25 to 300ºC. A

decrease in conductance with temperature is clearly observed. A change in the shape of the curve at the resonance is also noticed when temperature increases. The appearance of a second peak on the curve can lead to wrong measurement interpretation. For instance, if we pay attention to the peaks at 383.2 MHz on Figure 1, we can't establish the value of the temperature.

This phenomenon is due to the modification of directivity properties as shown in Figure 2. Indeed, directivity d expresses the energy distribution in the cavity created by the two Bragg mirrors. If $d = 0^o$, the energy is concentrated at the beginning of the stopband. On the contrary, if $d = 90^o$, the energy is mostly located at its end. As a consequence, when directivity evolves, as shown Figure 2, the shape of the sensor response is modified. This can be seen on Figure 1 : the device is designed to work at the beginning of the Bragg band. But, when temperature (so d) changes, the energy tends to move in the Bragg band. As the band is narrow in this device, this lead to the splitting of the peak.

Moreover, the reflection coefficient r is deeply linked to directivity as explained in [8]. It is well known by men of the art that the control of reflection coefficient is a critical criteria to design SAW systems. The collapse of r and the modifications of d with temperature (Figure 2) also induce the decrease of insertion losses when heat rises.
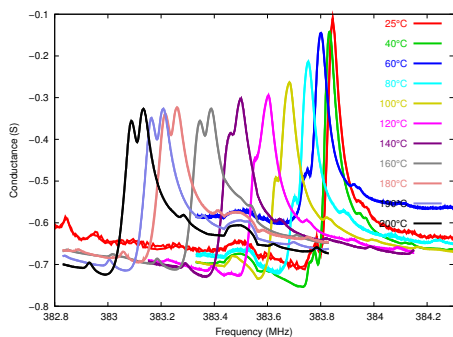

Figure 1. Evolution of the electrical response of a resonator on langasite (YXlt)/48.5/26.7^o on a temperature range from 25 to 300°C to reveal directivity effects

B. *Spectral quality of a three strips per wavelength resonator*

To exhibit that a structure working out of the Bragg band can be used to remove the influence of directivity on the system, the behavior of a wave propagating under an infinite grating of platinum made of three strips per wavelength λ is studied (transducer Figure 4. Once again, a langasite (YXlt)/48.5/26.7^o cut substrate is selected to put forward that contrary to the results of section II-A and despite the existence of two phase/frequency conditions involving the synchronism of the design, either the beginning or the end of the Bragg band is inhibited. That is to say, directivity has a negligible effect on the response of the structure.

The observations to be drawn from the results represented on Figure 3 are :

- the large frequency gap between the first and the second contributions (about 8 MHz) that can be noticed when looking at the x-axis of Figures 3a and 3b;
- the very low electromechanical coupling (near to zero for all the temperatures considered on Figure 3) of the second resonance (high frequencies).
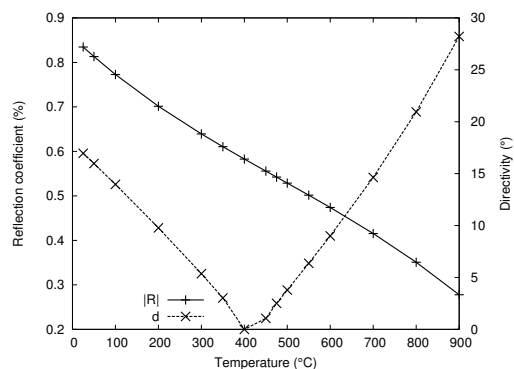

Figure 2. Theoretical estimation of the evolution of directivity and Rayleigh wave reflection properties under platinum electrode grating on langasite (YXlt)/48.5/26.7^o cut

The mechanical coupling can be deduced from these graphs considering the frequency gap between the resonance (maximum of admittance) and the antiresonance (zero of admittance, which is also the maximum of impedance). On these figures, susceptance and reactance are considered instead of admittance and impedance because the behavior of the structure is simulated by taking no losses into account.

These two assessments can be compared to the results of Figure 1 : as the two modes are well separated, a splitting of the principle mode in two is no more possible. Moreover, the very low coupling of the second resonance induces that this mode will not perturb the first one.

This first result, obtained considering an infinite grating of electrodes, demonstrates that benefits are brought by working out of the Bragg conditions, especially the possibility to cancel the effects of directivity. As a consequence, a resonator can now be designed according to the previous results and following the pattern described on Figure 4.

The design of this kind of structures involves new criteria and depends on the parameter to promote (coupling factor, low cavity modes, etc.). The operating point is selected according to the specifications. Regarding these considerations, three cases are considered. Table I recaps their dimensions. The frequency response functions of these structures are plotted from Figure 5 to Figure 7. In first instance, the device is designed so that the resonant frequency (synchronous frequency) is on the edge of the bandgap. The second case presents a synchronous frequency between the beginning and the middle of the bandgap. Finally, this frequency is located in the center of the bandgap. We can notice that the use of one or another location solution involves a trade-off between design criteria. For example, the first case shows a good dynamic on the reflection coefficient S_{11} (y-axis of Figures 5a, 6a, 7a) but, the best ratio of cavity peaks on principal peak appears in the third case, as for the best coupling factor than can be determined on Figures 5b, 6b, 7b by considering the distance between the maximum of conductance and its zero.

Finally, despite a low coupling factor (about 0.1% whereas a similar structure working in the Bragg band has got a coupling factor of about 0.25%) a resonator with a frequency response function that meets the spectral purity requirements has been successfully designed.
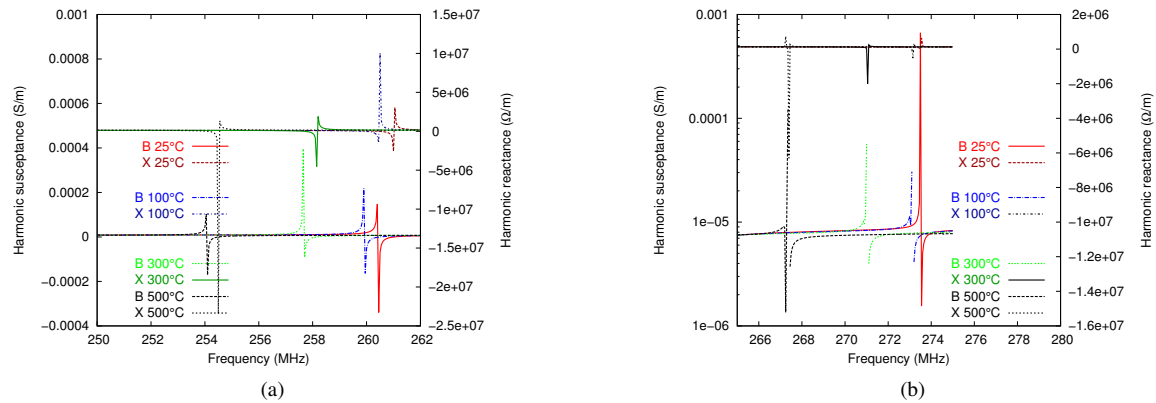
Figure 3. Rayleigh wave admittance on langasite (YXlt)/48.5/26.7º cut propagating under a platinum grating (harmonic analysis) for three electrodes per wavelength. (a) main contribution at "low" frequencies, (b) marginal contribution at high frequencies
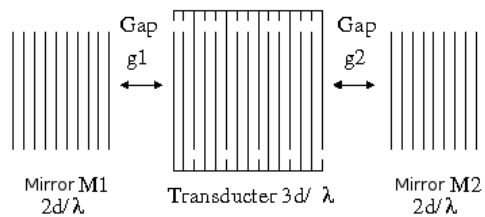

Figure 4. Schematic of a three strips per wavelength resonator

TABLE I. DESIGN TECHNOLOGICAL PARAMETERS OF THE THREE SIMULATED DEVICES

Parameters	Device Figure 5	Device Figure 6	Device Figure 7
number of electrodes (transducter: IDT)	900	900	900
IDT mechanical period (μm)	1.97	1.968	1.965
a/p (IDT)	0.5	0.5	0.5
h/λ (IDT)	2.369%	2.371%	2.375%
number of electrodes in a mirror	150	150	150
Mirror period (μm)	2.924	2.924	2.924
a/p (mirrors)	0.53	0.53	0.53
h/λ (mirrors)	2.394	2.394	2.394
Gap g1 (μm) / (g2=0μm)	1.15	1.8	1.8
acoustic opening (μm)	300	300	300
electrode height (nm)	140	140	140

C. Remarks on designs

Three remarks can be added to the previous results. Indeed, computations showed that the nearer your are from the pure periodical excitation (alternating of +V/-V), the more the secondary frequency contribution appears and the more losses at the synchronous frequency are intensified. For instance, a device with an excitation of floating/-V/+V/-V/floating/+V/-V/+V will have a better spectral purity that a device with +V/-V/+V/+V/-V/+V/-V excitation. To put it in a nutshell, the response of the SAW device is better if the excitation pattern is far from the +V/-V pattern.

Then, the design of resonators pointed out the possibility to obtain purified designs with a prevailing mode in spite of the multimodal character of the cavity.

Moreover, this kind of structure is easier to manufacture than a three electrodes per λ system (larger strips to reach the same frequency). Thanks to these two advantages, a $5/2\lambda$ electrodes structure would be preferred than the $3/\lambda$ electrodes system, which was presented at the beginning of the paper.

III. MULTIPLE MODE RESONATORS

Now that the possibility to remove the influence of the directivity on a SAW system response while keeping a good spectral purity as been demonstrated, we will focus our attentions on the possibility to design a monolithic temperature sensor to free the system from the problematics presented during the introduction. Consequently, the multimodal character of the cavity is exploited.

A. Demonstration of the possibility to design a monolithic SAW sensor

In the previous section, a single gap was taken into account in order to simplify the optimization of the electrical response. Now, two gaps are considered, as depicted on Figure 4. They are defined so that several resonances can exist in the wanted frequency range. To sum up, an acoustic cavity is created between the two Bragg mirrors. A transducer takes place inside this cavity that benefits from the energy of the cavity and interrogates it thanks to direct and inverse piezoelectric effects.

Such a configuration is an effective way to design a temperature sensor using only one resonator by putting several resonances in the ISM band. Indeed, the small variations of the frequency difference between the peaks can be measured. A SAW component is consequently designed. Its dimensions are determined to obtain two main modes well separated and with a maximum frequency interval between these two resonances. A langasite substrate is still used and electrodes are made of platinum. The structure of this component is summarized in table II and its frequency response at ambient is given Figure 8.

The frequency difference Δf between two resonances (f_b and f_a) can be numerically evaluated. Indeed, an harmonic analysis performed on a periodic and infinite electrodes grating reveals a phase velocity v_φ of about 2585 m/s. Considering the values given in table II, we can deduce the total length of the resonator: $L_c \simeq 915\lambda_{ac}$ with λ_{ac} the wavelength of the transducer. As a consequence:

$$\Delta f = f_b - f_a = \frac{v_\varphi}{2L_c} \simeq 236\text{KHz with } f_b > f_a \qquad (1)$$

(a)

(b)
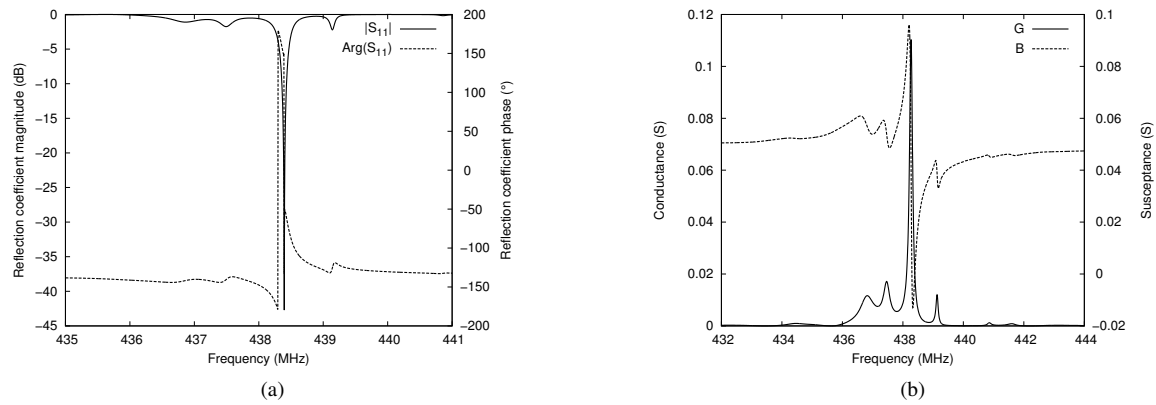
Figure 5. Electric response of a resonator that works on the edge of the bandgap - (a) reflection coefficient s_{11}, (b) admittance Y

(a)

(b)
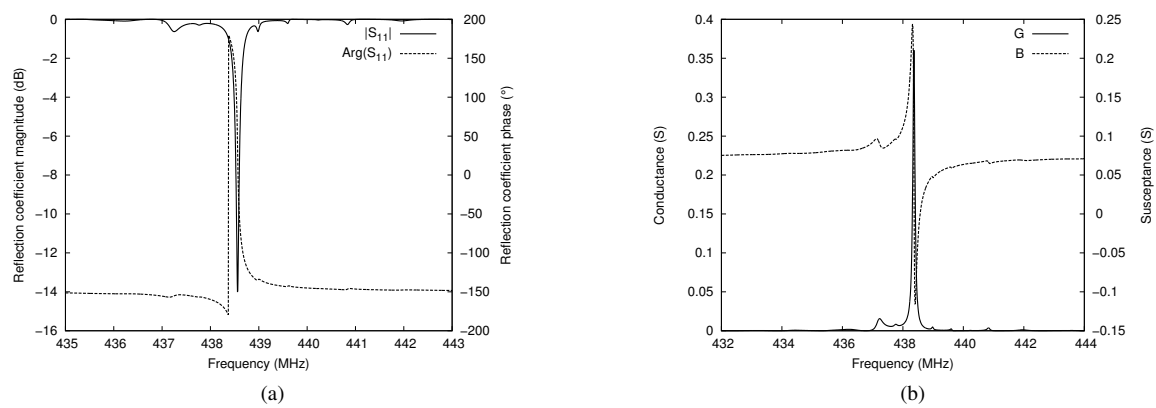
Figure 6. Electric response of a resonator that works between the beginning and the middle of the bandgap - (a) reflection coefficient s_{11}, (b) admittance Y

(a)

(b)
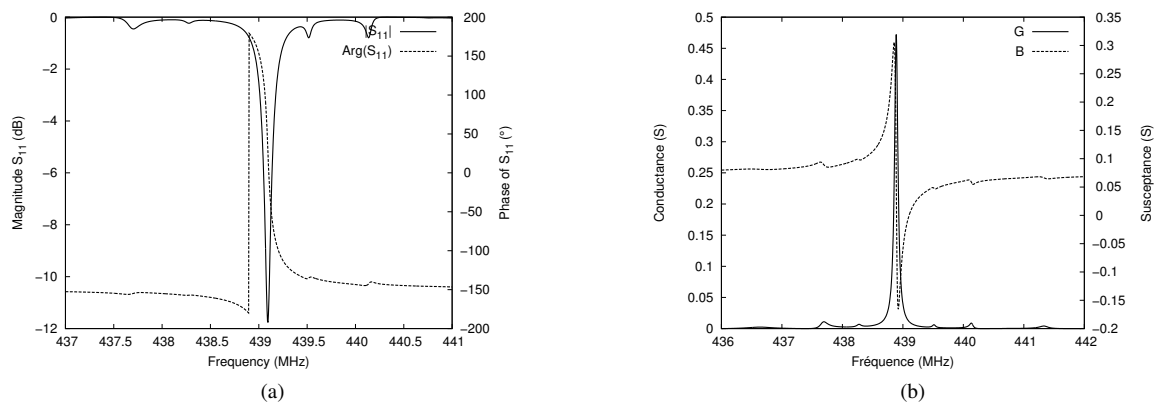
Figure 7. Electric response of a resonator that works in the middle of the bandgap - (a) reflection coefficient s_{11}, (b) admittance Y

The previous equation is not entirely exact. Indeed, the total length of the device is considered to take into account the probability density of the presence of a mode. But, if the mirrors were perfect, only the acoustic cavity should be taken into account. However, it can be used as a first approximation to size the resonator. Then, this frequency difference evolves along temperature as follows:

$$\Delta(\Delta f) \quad = \frac{\partial(\Delta f)}{\partial v_\varphi}dv_\varphi + \frac{\partial(\Delta f)}{\partial L_c}dL_c \tag{2}$$

$$= \Delta f_0 \times \left(\frac{\Delta v_\varphi}{v_0} - \frac{\Delta L_c}{L_0}\right) \tag{3}$$

with $\Delta(\Delta f)$ that expresses the variation of the frequency gap between two temperatures ; Δf_0 (resp. v_0, resp. L_0) is the frequency gap (resp. the wave velocity, resp. the length of the cavity) at the initial temperature. Terms in (2) correspond to

the total exact differential of Δf.

Moreover, the variations of the wave velocity and of the length of the cavity versus temperature have been established by Bechmann and al. [9]. They are here expressed at the second order :

$$\frac{\Delta v_\varphi}{v_0} = CTV_1(T - T_0) + CTV_2(T - T_0)^2 \qquad (4)$$

$$\frac{\Delta L_c}{L_0} = \alpha_1^{(1)}(T - T_0) + \alpha_1^{(2)}(T - T_0)^2 \qquad (5)$$

Finally, as $CTV_2 \ll CTV_1$, the variation with the temperature of the frequency difference can be approximated by:

$$\frac{\Delta(\Delta f)}{\Delta f_0} = (CTV_1 - \alpha)(T - T_0) \qquad (6)$$

The CTV and the first order dilatation coefficient α for the (YXlt)/48.5/26.7° cut of Langasite were determined by Bungo and al. [10]. It has been shown that $CTV_1 = -12.6 ppm.K^{-1}$, $CTV_2 = 73.9 ppb.K^{-1}$ and $\alpha = 5 ppm.K^{-1}$. As a consequence, the calculation (as described in this section) of the frequency gap of this device between 100°C and 200°C is assumed to be 2.175 kHz if the initial frequency difference is 680 kHz. This is consistent with the results of the numerical simulations, which give a Δf of 2 kHz (Figure 9). Otherwise, in this LGS crystal cut, reflection and conduction losses rise fast with temperature, so the design has to be improved: both variation of the frequency gap at these temperatures and losses due to the fall of reflection and transducer coefficients can be seen. Nevertheless, despite the high losses due to the increase of temperature, the good correlation between expected frequency variations and simulation results have shown the interest of our approach to measure temperature: a monolithic SAW sensor has been designed.

TABLE II. DESIGN TECHNOLOGICAL PARAMETERS OF A FOUR PEAKS RESONATOR

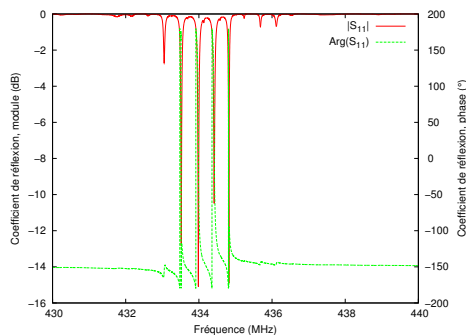| Parameters	Device
number of wavelengths (transducter: IDT)	100
IDT mechanical period (μm)	1.989
number of electrodes in a mirror	200
Mirrors mechanical period (μm)	2.973
a/p (IDT & mirrors)	0.5
h (nm)	118
acoustic aperture (μm)	300
Left gap (μm)	994.5
Right gap (μm)	1990

Figure 8. Reflexion coefficient s_{11} of a multiple mode resonator designed on langasite in the ISM band associated to the structure described table II
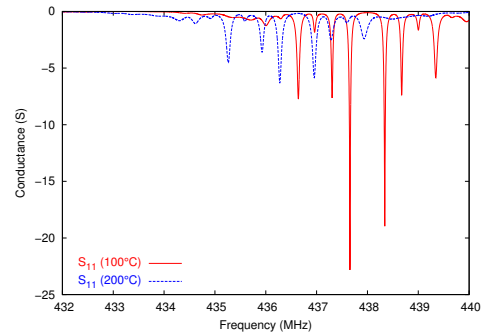

Figure 9. Frequency response of the device described table II designed on Langasite (YXlt)/46.5/26.7° with platinum electrodes for two different temperatures.

B. *Experimental results*

Finally, a monolithic temperature SAW sensor is manufactured to validate the previous results. A Quartz substrate and aluminum electrodes are used. The transducers are made of three strips per wavelength and three resonances in the ISM band are expected. The evolution of the frequency gaps is studied from 25°C to 130°C. The measures are done thanks to a wafer probe whose chuck heats in this temperature range.

Figure 10 shows the frequency response of this device for different temperatures. The frequencies are normalized. The shift of the three resonances due to temperature changes can be clearly observed on this graph. Furthermore, if we have a look at Figure 11, we can study the evolution of the frequency gap between the first and the last resonances along temperature. A decline of the normalized frequency difference with temperature can clearly be observed. Indeed, the frequency gap evolution under a temperature change can be approximated by the following law :

$$\frac{\Delta(\Delta f)}{\Delta f_0} = CTF_1(T - T_0) + CTF_2(T - T_0)^2 \qquad (7)$$

with $CTF_1 = -102$ppm/°C and $CTF_2 = 226.5$ppb/°C.

These results are consistent with the previous theoretical analysis: a structure composed of an only transducer made of a three electrodes per wavelength pattern was designed. The response of this resonator shows three resonances whose frequency difference of one peak to another decreases when temperature increases.

As a consequence, after a set of calibrations, this device is ready for use as a monolithic temperature sensor, which won't be subject to inconvenience such as frequency jumps due to a change in directivity. Moreover, as a monolithic sensor, it will not be subject to different aging between the different structures.

IV. CONCLUSION

Finally, this paper described a new design for surface acoustic wave devices to mitigate the effects of the splitting of the mode due to directivity effects and to raise the issue of the badly known interaction between the resonators forming the sensor.

As a consequence, a structure on LGS whose transducer works out of the Bragg band is proposed. By this way, the shape of its response function is no more impacted by the
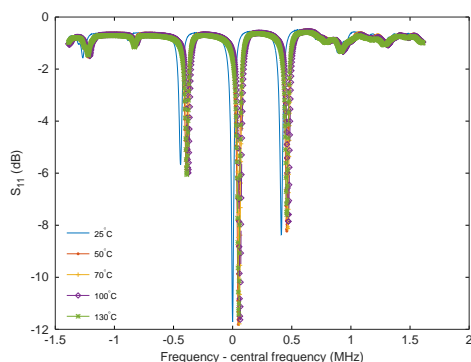
Figure 10. Reflexion coefficient s_{11} of a multiple mode resonator on Quartz substrate with aluminum electrodes. This figure shows the behavior of the three resonances when temperature varies for 25^oC to 130^oC
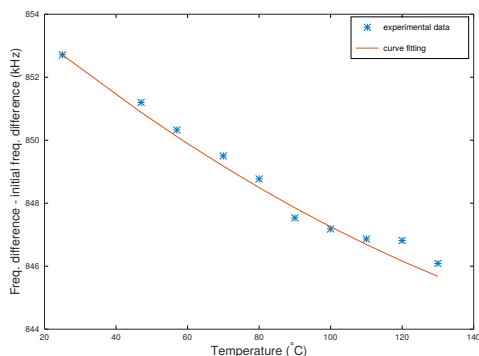

Figure 11. Evolution of the frequency gap between the first and the third resonance with temperature.

directivity while keeping a good spectral purity, which is required for resonators and sources.

Furthermore, the intrinsic multimodal character of the acoustic cavity is turned to its advantage. Indeed, a single resonator with three main resonances was designed so that differential measurements can be conducted to monitor environmental parameters. To validate this theoretical model, a three strips per wavelength structure was realized on a Quartz substrate. The possibility to monitor the evolution of temperature between 25 and 130^oC was demonstrated.

Further works will highlight the good agreement between theoretical and experimental results on LGS.

REFERENCES

[1] L. M. Reindl and I. M. Shrena, "Wireless measurement of temperature using surface acoustic waves sensors," IEEE Transactions on Ultrasonics, Ferroelectrics, and Frequency Control, vol. 51, no. 11, Nov 2004, pp. 1457–1463.

[2] M. P. da Cunha, A. Maskay, R. J. Lad, T. Coyle, and G. Harkay, "Langasite 2.45 GHz ISM band SAW resonator for harsh environment wireless applications," in 2016 IEEE International Ultrasonics Symposium (IUS), Sept 2016, pp. 1–4.

[3] W. Buff, M. Rusko, E. Goroll, J. Ehrenpfordt, and T. Vandahl, "Universal pressure and temperature SAW sensor for wireless applications," in 1997 IEEE Ultrasonics Symposium Proceedings. An International Symposium (Cat. No.97CH36118), vol. 1, Oct 1997, pp. 359–362 vol.1.

[4] H. Tan, X. Chen, J. Ma, and Y. Tan, "A design of substation temperature online monitoring system based on SAW temperature sensor," in 2016 IEEE International Conference on High Voltage Engineering and Application (ICHVE), Sept 2016, pp. 1–4.

[5] M. Born et al., Principles of Optics: Electromagnetic Theory of Propagation, Interference and Diffraction of Light, 7th ed. Cambridge University Press, 1999.

[6] F. Sidek, N. A. Ramli, A. N. Nordin, and I. Voiculescu, "Design and fabrication of Surface Acoustic Wave resonators on Lithium Niobate," in 2010 IEEE Student Conference on Research and Development (SCOReD), Dec 2010, pp. 343–347.

[7] P. Ventura, P. Dufilie, and S. Boret, "The effect of the fabrication process in propagation and reflectivity in an IDT," in 1996 IEEE Ultrasonics Symposium. Proceedings, vol. 1, Nov 1996, pp. 281–284 vol.1.

[8] P. Ventura and J. M. Hode, "A new accurate analysis of periodic IDTs built on unconventional orientation on quartz," in 1997 IEEE Ultrasonics Symposium Proceedings. An International Symposium (Cat. No.97CH36118), vol. 1, Oct 1997, pp. 139–142 vol.1.

[9] R. Bechmann, A. D. Ballato, and T. J. Lukaszek, "Higher-Order Temperature Coefficients of the Elastic Stiffnesses and Compliances of Alpha-Quartz," Proceedings of the IRE, vol. 50, no. 8, Aug 1962, pp. 1812–1822.

[10] A. Bungo et al., "Analysis of Surface Acoustic Wave Properties of the Rotated Y -cut Langasite Substrate," Japanese Journal of Applied Physics, vol. 38, no. 5S, 1999, p. 3239. [Online]. Available: http://stacks.iop.org/1347-4065/38/i=5S/a=3239